

As an alternative to Eq. (A1), the interaction may be expressed in terms of singlet-even and triplet-odd potentials [Eqs. (8) and (9)]. The matrix elements of the interaction in this form are given in Eqs. (10a) and (10b). The \bar{A} 's, \bar{B} 's, and \bar{M} 's can be simply expressed as linear combinations of the quantities calculated in Eq. (A4),

$$\bar{A}_0 = \frac{1}{4}(A_0 + A_1 - A_2 - A_3)$$

and

$$\bar{A}_3 = \frac{1}{4}(3A_0 - 3A_1 + A_2 - A_3),$$

with identical expressions for \bar{B}_0 , \bar{B}_3 , \bar{M}_0 , and \bar{M}_3 .

Effect of Quadrupole Collective Motions on the Giant Dipole Resonance*

A. K. KERMAN AND HO KIM QUANG†

*Laboratory for Nuclear Science and Physics Department, Massachusetts Institute of Technology,
Cambridge, Massachusetts*

(Received 25 March 1964)

The photonuclear model which includes both scalar and tensor polarizabilities is refined by considering small vibrations of the nuclear shape deformation. The effects of these zero-point vibrations on the structure of the giant dipole resonance for elastic and inelastic scattering have been investigated in an adiabatic approximation. Illustrations are given.

I. INTRODUCTION

IT has been established experimentally that there is a definite correlation between the giant dipole resonance of the photonuclear effect and nuclear deformation. These resonances are appreciably narrower in the closed-shell nuclei than those found in nuclei situated between closed shells. For deformed nuclei, the giant resonances broaden and even split into two peaks; this is especially apparent in the rare-earth region where the deformation is particularly large. For an ellipsoidal nucleus having a positive intrinsic quadrupole moment, the higher energy resonance is observed to contain about twice as much area as the lower energy resonance, the latter being always sharper than the narrowest resonances found in spherical nuclei.

These results are all in accord with the predictions of Okamoto¹ and Danos² that for a deformed nucleus the dipole oscillations would take place with two characteristic frequencies associated with the nuclear axes. The order of magnitude of the ratio of these frequencies follows from dimensional considerations, namely, $\omega_1/\omega_2 = 0.91R_2/R_1$ as given by a detailed hydrodynamic analysis, where R_1 and R_2 are the largest and smallest radii of the nucleus. Recently Fano,³ and Fuller and Hayward,⁴ using tensorial techniques, derive a more

general theory which takes into account the dependence of the photon scattering upon the spin orientation of the nucleus with respect to the wave vector of the photon, and thus includes three possible polarizability contributions: scalar, vector, and tensor.

Many experimental absorption data of strongly deformed nuclei seem to agree as well with the three-resonance theory first proposed by Inopin.⁵ On the basis of the hydrodynamic model within the framework of the theory of axially asymmetric nuclei proposed by Davidov and Filippov, Inopin showed that the resonance energies E_i corresponding to the density oscillations along the three different axes are proportional to $1/R_i$. Any experimental results for deformed nuclei can thus be interpreted by a three-line fit, for which two resonance energies E_1 and E_2 may be allowed to approach each other at a common value E_{12} . However, we know that a nonaxial deformation is generated by shape vibrations away from equilibrium axial symmetry, so called γ vibrations, and it seems sensible to assume that these vibrations might make more or less important contributions to the photoeffect resonance.⁶

Those considerations motivate us to include, if only for the sake of self-consistency of the collective model, zero-point vibrations of the nuclear shape. Conversely a successful interpretation of some aspects of the photonuclear effect on this basis might be useful in the study of nuclear structure, in revealing properties of collective levels and estimates of the zero-point vibra-

* This work is supported in part through U. S. Atomic Energy Commission Contract AT (30-1)-2098.

† Based upon a thesis submitted by H. K. Q. to the MIT Physics Department in partial fulfillment of the requirements for the Master of Science degree, August 1963.

¹ K. Okamoto, *Phys. Rev.* **110**, 143 (1958).

² M. Danos, *Nucl. Phys.* **5**, 23 (1958).

³ U. Fano, *Natl. Bur. Std. (U. S.) Tech. Note* **83**, (1960).

⁴ E. Fuller and E. Hayward, *Nucl. Phys.* **30**, 613 (1962).

⁵ E. Inopin, *Zh. Eksperim i Teor. Fiz.* **38**, 992 (1960) [English transl.: *Soviet Phys.—JETP* **11**, 714 (1960)].

⁶ P. A. Tipler, P. Axel, N. Stein, and D. C. Sutton, *Phys. Rev.* **129**, 2096 (1963).

tions. Recently Danos and Greiner⁷ have developed a dynamical model of the giant resonances in heavy deformed nuclei in which the coupling between the dipole oscillations and the quadrupole vibrations is treated adiabatically. They have showed in particular that the zero-point γ vibrations give an appreciable contribution to the pure giant resonance. Our work offers an alternative treatment of the problem for both spherical and deformed nuclei.

II. THE SCATTERING OPERATOR IN THE ADIABATIC APPROXIMATION

The scattering operator in the electric dipole approximation can be expressed as

$$f = \mathbf{r} \cdot \hat{\lambda} (H + \hbar\omega)^{-1} \mathbf{r} \cdot \hat{u} + \mathbf{r} \cdot \hat{u} (H - \hbar\omega')^{-1} \mathbf{r} \cdot \hat{\lambda}, \quad (1)$$

where the different factors are defined as follows: \mathbf{r} , radius vector from the center of mass of a nucleus to the center of its charge; $\hbar\omega$, $\hbar\omega'$, energies of the incident and scattered photons; $\hat{\lambda}$, \hat{u} , unit polarization vectors of the incident and scattered photons. In the energy denominators we will assume that the ground-state energy of the nucleus is taken to be zero and the Hamiltonian operator, when operating on the intermediate states, introduce imaginary parts to take account of the damping effects. In (1) other possible contributions, such as Thompson and Delbruck scatterings, have not been considered; their inclusion would not affect in any way the conclusions of the present study.

We shall be using an adiabatic approximation to calculate the scattering. That is to say, we make use of the fact that the time for the giant dipole scattering, which is characteristic of many MeV, is much shorter than the time for collective motions, which are characterized in general by less than one MeV. This means that we can first calculate the scattering with the system frozen as far as collective motions are concerned. Then the elastic scattering and the inelastic scattering to the collective states will be given as matrix elements of the scattering operator taken over the collective coordinates. For the case of quadrupole collective motions the convenient coordinates are those used by Bohr,⁸ i.e., the deformation parameters β and γ and the Euler angles θ_i . The scattering can then be calculated for a fixed β , γ , and θ_i .

The above operator f can be written in the intrinsic nuclear coordinate system as

$$f = \sum_i \lambda_i \mu_i A_i, \quad (i=1, 2, 3), \quad (2)$$

where

$$A_i = \langle \beta\gamma | r_i | i \rangle \left\{ \frac{1}{E_i + \hbar\omega + i\hbar\gamma_i} + \frac{1}{E_i - \hbar\omega - i\hbar\gamma_i} \right\} \times \langle i | r_i | \beta\gamma \rangle, \quad (3)$$

where $|\beta\gamma\rangle$ stands for the intrinsic wave function of the

system for fixed values of β and γ , and where the energies of the incident and scattered photons have been assumed to be equal.

The presence of only one type of intermediate state $|i\rangle$ in the expression (3) is a consequence of the basic assumption made in this study and in the preceding ones. That is to say that each of the three operators r_i will excite a giant dipole resonance characteristic of the motion along the axis i . Of course these are not eigenstates of the system and the widths which occur in the denominator are meant to take account of the damping to more complicated motions. In the absence of better information we shall assume that the three γ_i are equal. The energies E_i will of course depend on i and in fact this will be the main point at which the dependence of f on β and γ can enter. The matrix elements $\langle \beta\gamma | r_i | i \rangle$ can be written down explicitly if we assume that the oscillator strength in the present model is $NZ\alpha/A$, where the factor $\alpha \simeq 1.4$ takes account of the effects of the exchange forces in the nucleus

$$|\langle \alpha\beta | r_i | i \rangle|^2 = (\hbar^2/2ME_i)(NZ/A)\alpha.$$

Returning now to Eq. (2), we re-express f in spherical coordinates as follows:

$$f = \sum_{\nu} [(-)^{\nu} \lambda_{\nu} \mu_{-\nu} A_{\nu} + \lambda_{\nu} \mu_{\nu} A_{\nu}'], \quad (4)$$

$$\nu = -1, 0, +1,$$

$$A_0 = A_z, \quad A_0' = 0,$$

$$A_+ = A_- = \frac{1}{2}(A_x + A_y) \quad A_+' = A_-' = \frac{1}{2}(A_x - A_y).$$

A simple transformation will give the polarization vector products in terms of the polar angles (θ, ϕ) referred to the laboratory fixed axes:

$$\lambda_{\nu} \mu_{-\nu}(\theta' \phi') = \sum_{j\sigma} T_{j\sigma}(\theta\phi) D_{\sigma 0}^j(\theta_i) C(11j; \nu - \nu), \quad (5)$$

$$\lambda_{\nu} \mu_{\nu}(\theta' \phi') = \sum_{j\sigma} T_{j\sigma}(\theta\phi) D_{\sigma, 2\nu}^j(\theta_i) C(11j; \nu\nu), \quad (5')$$

with

$$T_{j\sigma}(\theta\phi) = \sum_M C(11j; M\sigma - M) \lambda_{\sigma - M\mu M}(\theta\phi). \quad (6)$$

The angular dependence of the scattering is given entirely by the tensor $T_{j\sigma}(\theta, \phi)$ from which the angular distribution corresponding to different values of the angular momentum transfer j can be calculated. If we restrict ourselves exclusively to the cases where the incident gamma rays are unpolarized, and no polarization analysis is made after scattering, the angular dependence can be expressed in simple forms³

$$G_j(\theta, \phi) = \sum_{\sigma} T_{j\sigma} T_{j\sigma}^* = \frac{1}{6}(1 + \cos^2\theta), \quad j=0$$

$$= \frac{1}{2}(2 + \sin^2\theta), \quad j=1$$

$$= \frac{1}{12}(13 + \cos^2\theta), \quad j=2 \quad (7)$$

where θ is the photon scattering angle.

⁷ M. Danos and W. Greiner, Phys. Rev. **134**, B284 (1964).

⁸ A. Bohr, Kgl. Danske Videnskab. Selskab, Mat. Fys. Medd. **26**, 14 (1962).

We now reach the final form of f :

$$f = \sum_{j\sigma} T_{j\sigma}(\theta\phi) \{ D_{\sigma 0^j}(\theta_i) \alpha_j + \delta_{j2} (D_{\sigma 2^j}(\theta_i) + (-)^j D_{\sigma, -2^j}(\theta_i)) \alpha_j' \}, \quad (8)$$

$$\alpha_j(\beta, \gamma) = \sum_{\nu} (-)^{\nu} C(11j; \nu - \nu) A_{\nu}(\beta, \gamma), \quad (8')$$

$$\alpha_j'(\beta, \gamma) = C(11j; 11) A_1'(\beta, \gamma). \quad (8'')$$

This operator explicitly separates the three 2^j -pole polarizabilities, namely, scalar, vector, and tensor, which correspond, respectively, to the three possible values of the angular momentum transfer $j=0, 1, 2$. In the present formalism, as a direct consequence of symmetry properties of the Clebsch-Gordan coefficients, the vector contribution vanishes identically. In the second term of (8) the simple geometrical restriction $|2\nu| \leq j$ rules out the scalar and vector contributions leaving only the tensor term $j=2$.

f depends, on the one hand, on the geometrical factors of the scattering through the Clebsch-Gordan coefficients and the tensor $T_{j\sigma}$ and, on the other hand, on the various dynamical factors such as charge distribution, photon energy, and shape parameters through the functions A_j . The A_j in effect, can be considered as functions of β and γ through the resonance energies, which vary in inverse proportion to the radii associated with the corresponding axes. The proportionality constant is estimated to be $82r_0$ (MeV-F) with r_0 taken to be 1.2–1.4 F.

In the present context we assume that β and γ

oscillate about their equilibrium values β_1 and γ_1 . The equilibrium shape parameters β_1, γ_1 can be estimated in the first approximation by relations derived in the liquid-drop model, or more realistically by using measurements from Coulomb excitation experiments. The dependence on β, γ of f can then be simplified considerably by an expansion in powers of $(\beta - \beta_1)$ and $(\gamma - \gamma_1)$. Of course the equilibrium value of β for vibrating spherical nuclei is zero, and for deformed nuclei we will take the conventional view that γ oscillates about zero even though in some cases the amplitude is rather large.

III. QUADRUPOLE OSCILLATIONS IN NUCLEAR MODELS

The surface boundary of a nucleus in which only quadrupole deformation is considered may be represented by the expression

$$R(\theta', \phi') = R_0 \{ 1 + (5/16\pi)^{1/2} \beta [\cos \gamma (3 \cos^2 \theta' - 1) + 3 \sin \gamma \sin^2 \theta' \cos 2\phi'] \}, \quad (9)$$

where γ can take on values from 0 to $\frac{1}{3}\pi$, and β , denoting the total deformation, varies from $-\infty$ to $+\infty$. The above expression also gives the sizes of the three nuclear radii when θ', ϕ' assume appropriate values.

$$R_i = R_0 \{ 1 + (5/16\pi)^{1/2} \beta \cos(\gamma - i\frac{2}{3}\pi) \} \quad i=1, 2, 3. \quad (10)$$

A. Spherical Nuclei

The wave functions of the ground state, first excited state, and triplet states are given, respectively, by

$$\psi_0 = \frac{N_0}{(8\pi^2)^{1/2}} \exp(-\beta'^2); \quad N_0 = 1 / \left[\frac{\sqrt{\pi}}{2} \left(\frac{\beta_0}{\sqrt{2}} \right)^5 \right]^{1/2} \quad (11)$$

$$\Psi_1 = \frac{N_1}{(8\pi^2/5)^{1/2}} \alpha_{2M} \exp(-\beta'^2); \quad N_1 = 1 / \left[\frac{5}{4} \sqrt{\pi} \left(\frac{\beta_0}{\sqrt{2}} \right)^7 \right]^{1/2} \quad (12)$$

$$\Psi_{2J} = \frac{N_{2,J}}{[8\pi^2/(2J+1)]^{1/2}} \left\{ \left[\sum_m C(22J; mM-m) \alpha_{2m} \alpha_{2,M-m} \right] - \frac{\sqrt{5}}{4} \beta_0^2 \delta_{J,0} \right\} \exp(-\beta'^2);$$

$$N_{20} = 1 / \left[\frac{\sqrt{\pi}}{4} \left(\frac{\beta_0}{\sqrt{2}} \right)^9 \right]^{1/2}, \quad N_{22} = 1 / \left[\frac{5}{4} \sqrt{\pi} \left(\frac{\beta_0}{\sqrt{2}} \right)^9 \right]^{1/2}, \quad (13)$$

where the normalization constant N 's are associated with β - and γ -dependent parts only; the parts depending on the Eulerian angles θ_i are normalized separately. The variable β' is just the ratio (β/β_0) where $\beta_0^2 = (2\pi/BC)$ is related to the zero-point vibrations. The variables α_{2m} are given in terms of β, γ , and Θ in the usual manner.⁸

In the following, the function $A_j(\beta, \gamma)$ will be averaged over the various nuclear shapes using the above wave functions re-expressed in the intrinsic nuclear system.

This calls for the substitution of the shape variables α by the parameters β and γ , and the Euler angles θ_i .

The above wave functions apply to even nuclei. The wave functions for an odd A nucleus include in addition to the part describing the nuclear core of the general form (11), (12), and (13) another part representing the last uncoupled nucleon. The calculations for this case are similar to the calculations for an even-even nucleus and will not be considered further.

We now proceed to derive the probabilities of occur-

rence for the processes: (1) elastic scattering $0 \rightarrow 0$; (2) inelastic scattering $0 \rightarrow 2$ and $0 \rightarrow 0', 2', 4$. This can be done by taking the square of the magnitude of the scattering amplitude averaged over the variations of β and γ .

1. Elastic Scattering

The matrix element $\langle \psi_0 | f | \psi_0 \rangle$ yields just one term, $j=0$. We should note, however, that the presence of pure scalar or pure tensor is a consequence of the particular example we are taking, namely, nuclei with zero-spin ground state. For other cases with nonzero-spin ground state there is mixture of scalar and tensor polarizabilities. The differential elastic scattering cross section can now be obtained by squaring $\langle f \rangle$ and using the explicit expression $G_j(\theta)$ in (7):

$$\frac{d\sigma}{d\Omega}(0 \rightarrow 0) = \left(\frac{e}{c}\right)^4 \left(\frac{1 + \cos^2\theta}{6}\right) E^4 |\langle 0 | \mathcal{Q}_0 | 0 \rangle|^2, \quad (14)$$

where

$$\langle 0 | \mathcal{Q}_0 | 0 \rangle = N_0^2 \int_{-\infty}^{+\infty} d\beta \beta^4 \int_0^{\pi/3} d\gamma \sin 3\gamma \times e^{-2\beta^2/\beta_0^2} \mathcal{Q}_0(\beta, \gamma).$$

Using the definitions of A_i and A_i given previously, Eq. (14) can be reduced to the familiar form:

$$\frac{d\sigma}{d\Omega} = \left(\frac{e^2}{Mc^2} \frac{NZ}{A} \alpha E^2\right)^2 \left(\frac{1 + \cos^2\theta}{2}\right) \times \left| \langle 0 | \sum_{i=1}^3 \frac{E_i^2 - E^2 + \gamma_i^2 + i(2\gamma_i)E}{(E_i^2 - E^2 + \gamma_i^2)^2 + (2\gamma_i)^2 E^2} | 0 \rangle \right|^2.$$

We rediscover here the usual dipole angular distribution and the explicit fact that the oscillations along each of the directions transverse to the quantization axis ($\nu = \pm 1$) have the same "weight" as those along the longitudinal direction ($\nu = 0$). This is so because \mathcal{Q}_0 is an equal combination of the three.

The absorption cross section for an unoriented system is proportional to the imaginary part of the scattering amplitude in the forward direction.

$$\sigma_a = 4\pi\lambda \left\{ \frac{1}{\sqrt{3}} \left(\frac{e}{c}\right)^2 E^2 \langle 0 | \text{Im} \mathcal{Q}_0 | 0 \rangle \right\}. \quad (15)$$

2. Transition $0 \rightarrow 2$

The scattering amplitude for this process is obtained by taking the matrix element $\langle \Psi_1 | f | \Psi_0 \rangle$ which leads to

the cross section:

$$\frac{d\sigma}{d\Omega}(0 \rightarrow 2) = \left(\frac{e}{c}\right)^4 \left(\frac{13 + \cos^2\theta}{60}\right) \times E^4 |\langle 1 | \mathcal{Q}_2 | 0 \rangle + 2\langle 1 | \mathcal{Q}_2' | 0 \rangle|^2,$$

$$\langle 1 | \left\{ \begin{array}{c} \mathcal{Q}_2 \\ \mathcal{Q}_2' \end{array} \right\} | 0 \rangle = N_1 N_0 \int \beta^4 d\beta \int d\gamma \sin 3\gamma e^{-2\beta^2/\beta_0^2} \times \left\{ \begin{array}{c} \beta \cos \gamma \mathcal{Q}_2(\beta, \gamma) \\ \frac{\beta}{\sqrt{2}} \sin \gamma \mathcal{Q}_2'(\beta, \gamma) \end{array} \right\}. \quad (16)$$

The only contribution comes from the tensor term, $j=2$, which could be revealed in laboratory measurements by its almost isotropic angular distribution, $(13 + \cos^2\theta)/12$, and should characterize the experimental observation of the transition. Further, as a result of both geometry and deformation, expressed by the presence of the deformation parameters, $a_{20} = \beta \cos \gamma$ in the first integral and $a_{22} = a_{2,-2} = (1/\sqrt{2})\beta \sin \gamma$ in the second, all three directions do not contribute equally.

3. Transitions $0 \rightarrow 0', 2'$

The scattering amplitude for the transition to the two-phonon state with $J=4$ vanishes in accord with the usual conservation of angular momentum. For the transitions to the two other states, the cross sections are given by $J=0'$

$$\frac{d\sigma}{d\Omega} = \left(\frac{e}{c}\right)^4 \left(\frac{1 + \cos^2\theta}{6}\right) E^4 |\langle 20 | \mathcal{Q}_0 | 0 \rangle|^2, \quad (17)$$

where

$$\langle 20 | \mathcal{Q}_0 | 0 \rangle = N_0 N_{20} \int \beta^4 d\beta \int d\gamma \sin 3\gamma \times \left(\frac{1}{\sqrt{5}} \beta^2 - \frac{\sqrt{5}}{4} \beta_0^2\right) e^{-2\beta^2/\beta_0^2} \mathcal{Q}_0(\beta, \gamma),$$

$J=2'$

$$\frac{d\sigma}{d\Omega} = \left(\frac{e}{c}\right)^4 \left(\frac{13 + \cos^2\theta}{60}\right) E^4 |\langle 22 | \mathcal{Q}_2(\beta, \gamma) | 0 \rangle + \langle 22 | \mathcal{Q}_2'(\beta, \gamma) | 0 \rangle|^2, \quad (18)$$

$$\langle 22 | \left\{ \begin{array}{c} \mathcal{Q}_2 \\ \mathcal{Q}_2' \end{array} \right\} | 0 \rangle = N_{22} N_0 \int \beta^4 d\beta \int d\gamma \sin 3\gamma \times \left\{ \begin{array}{c} -(2/7)^{1/2} \beta^2 \cos 2\gamma \mathcal{Q}_2 \\ (2/7)^{1/2} \beta^2 \sin 2\gamma \mathcal{Q}_2' \end{array} \right\} e^{-2\beta^2/\beta_0^2}.$$

From these formulas it is expected that the transition probabilities for the processes $0 \rightarrow 0'$ and $0 \rightarrow 2'$ show features similar to those found in $0 \rightarrow 0$ and $0 \rightarrow 2$, respectively.

We should remark that these inelastic cross sections are only nonzero in virtue of the dependence of $A_2(\beta\gamma)$ and $A_2'(\beta\gamma)$ on β and γ . These functions have the properties that

$$\begin{aligned} A_2'(\beta\gamma) &= 0 & \text{at } \gamma=0, \\ A_2'(\beta\gamma) &= A_2(\beta\gamma) = 0 & \text{at } \beta=0, \end{aligned}$$

and if the resonant frequencies were independent of β and γ they would remain zero. This is where we have put the essential coupling between the dipole and quadrupole motions.

B. Deformed Nuclei

In strongly deformed nuclei it is possible to separate, in their energy spectra, excitations of the rotational type from those of the vibrational type. This experimental result corresponds to the separability of the wave function:

$$\psi(IMK; In_\beta In_\gamma) = ((2I+1)/8\pi^2)^{1/2} D_{MK}^I(\theta_i) \times f_{In_\beta}(\beta) g_{In_\gamma}(\gamma) \quad (19)$$

with the β and γ wave functions given by:

$$f_{n_\beta}(x) = N_{n_\beta} (\sqrt{\pi} 2^{n_\beta} n!)^{-1/2} e^{-2x-sx^2} H_n((2s)^{1/2} x); \quad x = (\beta - \beta_1)/\beta_1 \quad (20)$$

$$g_{n_\gamma}(\gamma) = N_{n_\gamma}' (\omega'\gamma^2/\hbar)^{3/4} |\kappa| e^{-\omega'\gamma^2/2\hbar} \times F(-\frac{1}{2}n + \frac{1}{2}|\kappa|; |\kappa| + 1; (\omega'\gamma^2/\hbar)), \quad (21)$$

where $H_n(Z)$ are the Hermite polynomials, $F(a; b; c)$ the confluent hypergeometric function, and two new parameters s and t depending, respectively, on the β and γ potential strengths p and q :

$$s = (p\beta_1^4/\hbar/B)^{1/2}, \quad t = (\beta_1/2\hbar)(9B)^{1/2}. \quad (22)$$

The derivations of transition probabilities proceed in the same way as before. In terms of the general wave function (19), the matrix element of f between the initial state ($I_0 M_0 K_0$) and the final state ($I_f M_f K_f$) can be obtained and leads to the cross section:

$$\begin{aligned} \frac{d\sigma}{d\Omega} &= \left(\frac{e}{c}\right)^4 \frac{E^4}{2I_f+1} \sum_i G_i(\theta) \{ |C(I_0 j I_f; K_0 0) \langle f | \alpha_j | 0 \rangle|^2 \\ &+ |C(I_0 j I_f; K_0 2) \langle f | \alpha_j' | 0 \rangle|^2 \}, \quad (23) \end{aligned}$$

where the notations for the matrix elements have the following meaning:

$$\begin{aligned} \langle f | \alpha_j | 0 \rangle &\equiv \langle n_\beta n_\gamma \kappa; f | \alpha_j | n_\beta n_\gamma \kappa; 0 \rangle \\ &= \int d\beta \int d\gamma 2\gamma f_f(\beta) g_f(\gamma) \alpha_j(\beta\gamma) f_0(\beta) g_0(\gamma). \quad (24) \end{aligned}$$

The formalism separates explicitly transitions between states of the same K from transitions between states of K 's differing by two units. The first type includes such processes as the scattering between levels of the

same rotational band ($n_\beta = n_\gamma = 0$), or scattering to levels of the first β vibrational band ($n_\beta = 1, n_\gamma = 0$), while the second describes, for example, scattering to the first γ vibrational band ($n_\beta = 0, n_\gamma = 1$). Further, as before, the vector contribution is completely absent and only the tensor polarizability contributes to the transition to the γ band. Finally, all processes which do not satisfy the "triangular" rule

$$|I_0 - j| \leq I_f \leq I_0 + j$$

vanish, which implies for example that transition from the initial states with $I_0 = 0$ to final states I_f are forbidden unless $I_f = j$, thus limiting the final spin I_f to the values 0 and 2.

In detail, for this simple case $I_0 = 0, I_f = j$, various cross sections are given by the following expressions: Elastic scattering: ($I_0 = K_0 = 0 \rightarrow I_f = K_f = 0$)

$$\frac{d\sigma}{d\Omega} = \left(\frac{e}{c}\right)^4 \left(\frac{1 + \cos^2\theta}{6}\right) E^4 |\langle 00 | \alpha_0 | 00 \rangle|^2. \quad (25)$$

Transition to the first excited state:

$$\frac{d\sigma}{d\Omega} = \left(\frac{e}{c}\right)^4 \left(\frac{13 + \cos^2\theta}{60}\right) E^4 |\langle 00 | \alpha_2 | 00 \rangle|^2. \quad (26)$$

Transition to the first β excited state ($0 \rightarrow K_f = 0, I_f = 0, n_\beta = 1$):

$$\frac{d\sigma}{d\Omega} = \left(\frac{e}{c}\right)^4 \left(\frac{1 + \cos^2\theta}{6}\right) E^4 |\langle 10 | \alpha_0 | 00 \rangle|^2. \quad (27)$$

Transition to the rotation on the first β excited state ($0 \rightarrow K_f = 0, I_f = 2, n_\beta = 1$):

$$\frac{d\sigma}{d\Omega} = \left(\frac{e}{c}\right)^4 \left(\frac{13 + \cos^2\theta}{60}\right) E^4 |\langle 10 | \alpha_2 | 00 \rangle|^2. \quad (28)$$

Transition to the first γ excited state ($0 \rightarrow K_f = 2, I_f = 2, n_\gamma = 1$):

$$\frac{d\sigma}{d\Omega} = \left(\frac{e}{c}\right)^4 \left(\frac{13 + \cos^2\theta}{60}\right) E^4 |\langle 01 | \alpha_2' | 00 \rangle|^2. \quad (29)$$

Absorption cross section:

$$\sigma_a = 4\pi\lambda \left\{ \frac{1}{\sqrt{3}} \left(\frac{e}{c}\right)^2 E^2 \langle 00 | \text{Im } \alpha_0 | 00 \rangle \right\}. \quad (30)$$

IV. DISCUSSION

In the form of $A(\beta, \gamma)$ expanded in powers of β , the zeroth-order term corresponds to a static spherical nucleus, while higher order terms introduce corrections due to shape vibrations.

As a numerical example we take Sm^{150} , an even-even nucleus located at the border of the region of strongly

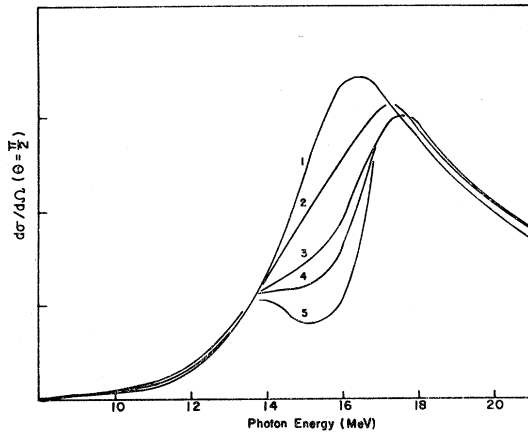


FIG. 1. Elastic scattering for Sm^{150} at 90° calculated for different values of the deformation β_0 . Curve 1 corresponds to the static shape, curve 3 corresponds to the correct value of $\beta_0=0.148$. The three other curves numbered 2, 4, and 5 give the predictions for $\beta_0=0.10, 0.17,$ and 0.20 , respectively.

deformed nuclei. In this transition region, the nucleus is particularly soft to positive parity vibrations. It has the first 2^+ level at 0.337 MeV and 0^+ level at 0.685 MeV. The following parameters are used in the numerical calculations:

Average radius	$R_0=5.4$ F,
Vibration amplitude	$\beta_0=0.148$,
Resonance energy	$E_r=16$ MeV,
Half-width	$\hbar\gamma=2.5$ MeV.

The elastic scattering curve (Fig. 1) shows that the second-order correction, proportional to β_0^2 lowers somewhat the maximum and increases contributions at the tails. The zero-point vibrations cause appreciable broadening of the resonance. For the value of $\beta_0=0.148$ calculated from the measured values of B_2 and C_2 ,⁹ this broadening $\Delta\Gamma/\Gamma$ is estimated to be of the order 40%. To show the relationship of the deformation to the width broadening, $\Delta\Gamma$ ¹⁰ is calculated for various values of β_0 (Fig. 2).

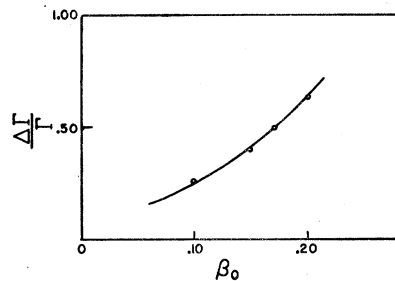


FIG. 2. Estimates of the width broadening of the resonance of photon-scattering from Sm^{150} for different assumed values of the total deformation of the target nucleus.

⁹ K. Alder, A. Bohr, T. Huus, B. Mottelson, and A. Winther, *Rev. Mod. Phys.* **28**, 432 (1956).

¹⁰ The width broadening $\Delta\Gamma$ is defined here and in the following by comparing, at half-width, the curve corresponding to the static shape with the curve in which β and γ vibrations are taken into account.

Letting the vibration amplitude increase we observe a second effect no less interesting: the curve around the resonance energy spreads and eventually splits

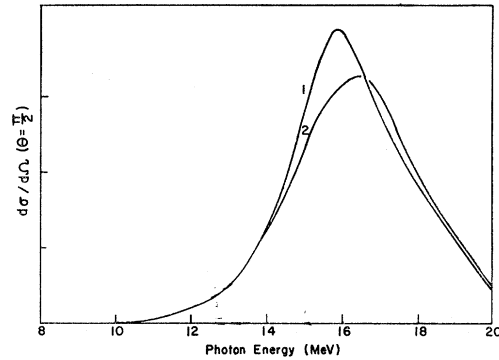


FIG. 3. Probability of transition to the first excited state of Sm^{150} for the first two orders in an expansion in powers of β .

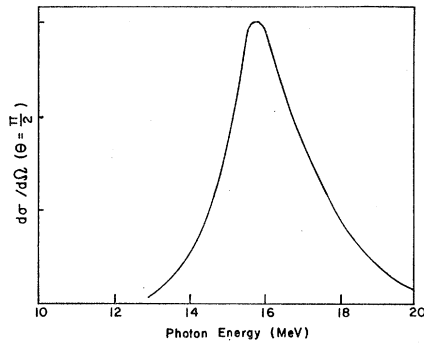


FIG. 4. Probability of transition to the zero-spin triplet state of Sm^{150} at 90° in the lowest order of the expansion in powers of β .

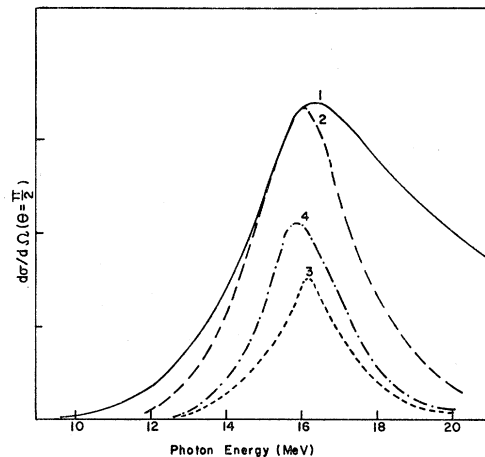


FIG. 5. Relative magnitudes of the probabilities of transition to different states of Sm^{150} at 90° . Curve 1 gives the predictions for elastic scattering. Curve 2 corresponds to transition to the first excited state, normalized for better comparison by multiplication with a factor of 3.77. The transition to the two-phonon states has much lower probability, as shown by curve 3 (transition to zero-spin level, normalized by a factor of 10) and curve 4 (transition to spin-two level, normalized by a factor of 100).

TABLE I. Effects of collective vibrations on the giant resonance for the case of Sm^{150} ($\beta_0=0.148$).

Transitions	Width broadening	Relative magnitudes
$0 \rightarrow 0$	40%	1
$0 \rightarrow 2$	40%	0.25
$0 \rightarrow 0'$		0.045
$0 \rightarrow 2'$		0.006

into two distinct maxima (Fig. 1). As the originally spherical nucleus becomes softer, it behaves more and more like an axially symmetrical deformed nucleus, and leads to the characteristic two peaked spectrum. Critical to the observation of this feature is the resonance width; if the latter is large enough, it can screen small variations with energy. So that, with good resolution measurements, the splitting of this photonuclear effect curve can serve as a criterion for shape deformation of the target nucleus.

The transition to the second 0^+ level (Fig. 4) which, it is recalled, depends only on the scalar term, varies essentially in the same ways, with the expected $(\beta_0)^2$ order of magnitude smaller, 4.5%.

Transitions to the spin-two states (Fig. 5) show markedly different features. For excitations to the first 2^+ level, the curve is considerably narrower than in the $0 \rightarrow 0$ case, by about 30%. The probability of occurrence rises sharply at resonance. At this point β vibration has a definite effect in lowering the curve. Similar effects may be observed in the transition to the second 2^+ level. As for the relative magnitudes of these transitions they vary as β_0 . The above results are summarized in Table I.

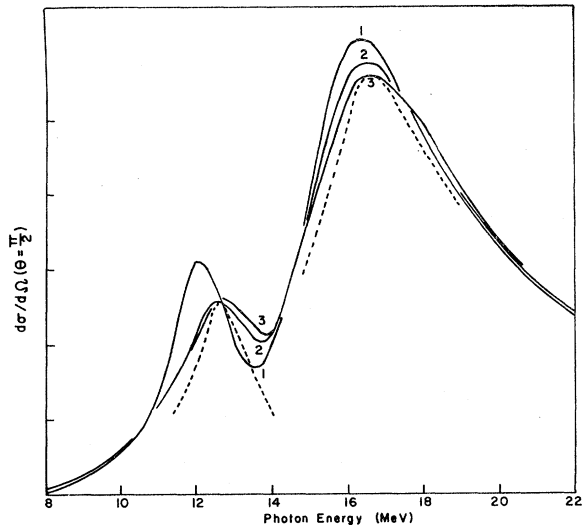


FIG. 6. Elastic scattering for Er^{164} at 90° . It is given by curve 1 for static deformation ($\beta_1=0.28$ and $\gamma_1=0$). The β vibrations lower the peaks and broaden the widths especially at the lower energy resonance (curve 2). Curve 3 shows the effects of γ vibrations together with β vibrations. The dashed curves, which correspond to static deformation, are drawn to facilitate comparison.

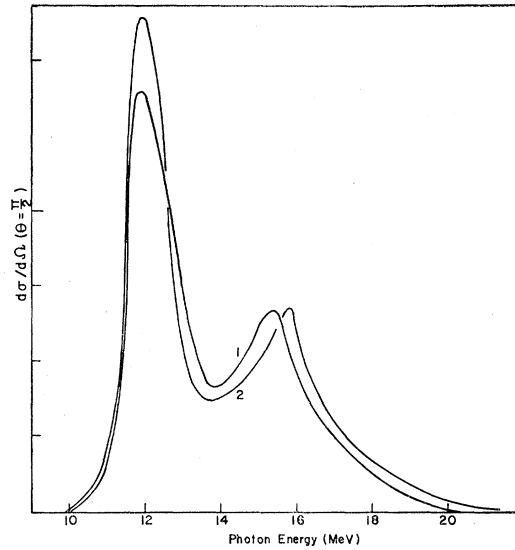


FIG. 7. Probabilities of transition to the first β excited state in Er^{164} in the two lowest orders.

As an example of a deformed nucleus we choose Er^{164} a rare-earth nucleus with a particularly large intrinsic deformation. The parameters used in the calculations are the following:

Average radius: 7.70 F,
 Resonance energies: $E_{12}=15.5$ MeV, $E_3=12$ MeV,
 Half-widths: $\hbar\gamma_{12}=2$ MeV, $\hbar\gamma_3=1$ MeV,
 Deformation parameters: $\beta_1=0.28$, $\gamma_1=0$,
 $s=3$, $t=17.82$ ($\gamma_{\text{rms}}=0.1676$).

In elastic scattering (Fig. 6), the cross section is lowered at peak-points by zero-point β vibrations; the width broadening hardly observable at the higher energy line ($\Delta\Gamma_3=13\%$), is more pronounced in

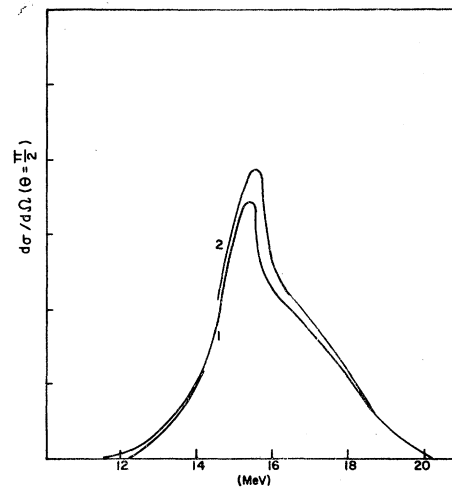


FIG. 8. Transition to the lowest state of the γ -vibrational band in Er^{164} in the two lowest orders.

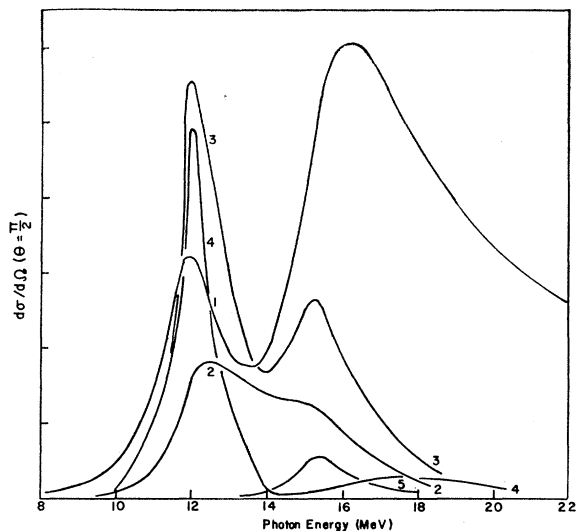


FIG. 9. Relative magnitudes of the probabilities of transition to different states of Er^{164} at 90° . The figure shows their very irregular variations with gamma energy. Curves 1 and 2 give the predictions of transition to the two lowest states of the ground-state band. Curves 3 and 4 correspond, respectively, to the two lowest states of the β vibration band, and curve 5 to the first γ vibrational state. The last three curves are normalized by a factor of 10 to facilitate comparison.

the lower energy line ($\Delta\Gamma_1=46\%$). These effects reflect the strong dependence of β vibrations on the energy corresponding to a classical oscillation along the symmetry axis. Zero-point γ vibrations also increase the

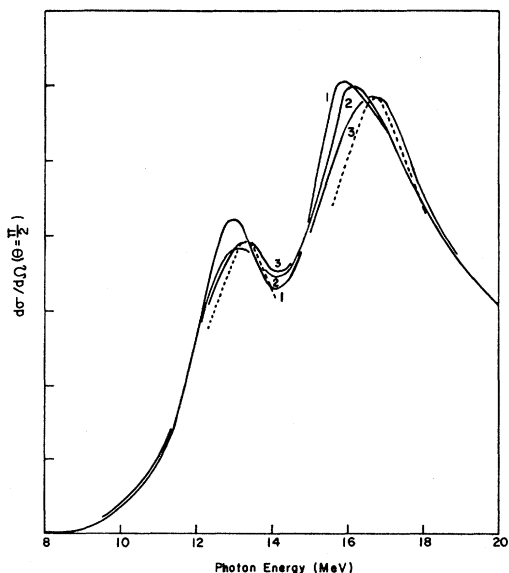


FIG. 10. Elastic scattering for Os^{188} at 90° . Curve 1 corresponds to static deformation ($\beta_1=0.20$ and $\gamma_1=0$); curve 2 shows the effects of β vibrations and curve 3 gives the predictions when γ vibrations are introduced. The dashed curves redraw the probability of transition for the case of static deformation. The effects of γ instability of the target nucleus can be seen by comparing this figure to Fig. 6.

energy spread of the higher energy ($\Delta\Gamma_3=22\%$, and $\Delta\Gamma_1=54\%$, for combined effects of β and γ in lowest orders). Even more significant is the shift to a higher energy of the low-resonance line: β and γ vibrations deform the nucleus in such a way that the contributions from oscillations along the symmetry axis become relatively larger.

The transition to the first excited level gives an idea how the tensor term would contribute to the elastic scattering since the two differ simply by a geometrical factor. The characteristic feature is that the two

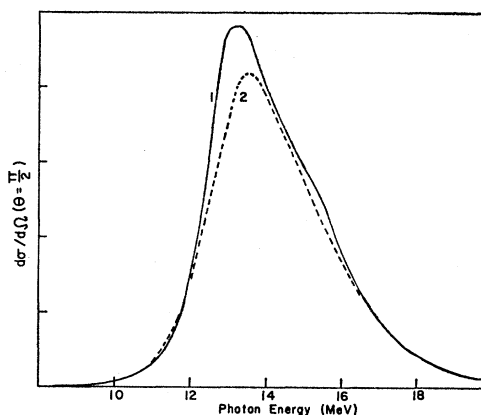


FIG. 11. Probability of transition to the first β excited state in Os^{188} in the two lowest orders.

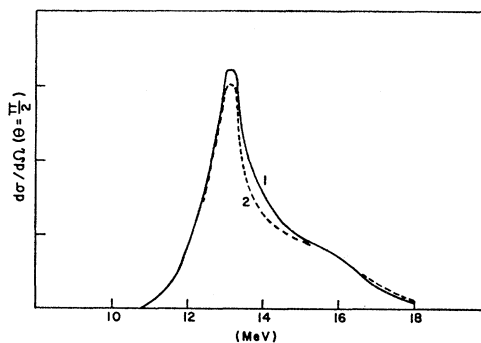


FIG. 12. Probability of transition to the first γ excited state in Os^{188} in the two lowest orders.

peak energies now largely spread can be no longer distinguished.

For transitions involving final β excited states, the first nonzero terms are linear in $(\beta-\beta_1)\partial A/\partial\beta$ and hence proportional to $R_i\partial R_i/\partial\beta$; the inequality $R_3 > R_1$ and the larger rate of change of R_3 with respect to β explain the difference in magnitudes at the two resonances. The widths are also observed to be narrower than in the above case. Zero-point vibrations seem to accentuate maxima and minima of the curve by amounts too small to be detected experimentally (Figs. 7-9).

The relative magnitudes of different transitions given in Table II vary irregularly, differing considerably at the resonance points.

As a final example we consider Os^{188} (Figs. 10–13) with which the periodic table finishes the deformed nucleus region to begin the transition region. It has an rms value of γ of about 19° , corresponding to a t value of 4.20.

Average radius: 6.85 F,
 Resonance
 energies: $E_1 = 15.50$ MeV, $E_3 = 12.75$ MeV,
 Half-widths: $\hbar\gamma_1 = 2$ MeV, $\hbar\gamma_3 = 1$ MeV,
 Deformation
 parameters: $\beta_1 = 0.20$, $s = 4.0$, $t = 4.20$.

TABLE II. Effects of collective vibrations in the case of a strongly deformed nucleus Er^{164} .

Transitions	Width broadenings		Relative magnitudes	
	$\Delta\Gamma_3/\Gamma_3$	$\Delta\Gamma_1/\Gamma_1$	at E_3	at E_1
$0 \rightarrow 0$	46% (β) 54% (γ)	14% (β) 22% (γ)	1	1
$0 \rightarrow 2$			0.56	0.22
$0 \rightarrow 0'$ (β)			0.17	0.044
$0 \rightarrow 2'$ (β)			0.15	0.005
$0 \rightarrow 2''$ (γ)			0	0.010

TABLE III. Width broadening of the giant resonances in some deformed nuclei due to collective quadrupole oscillations.

	γ	$\bar{\beta}$	$\Delta\Gamma_3/\Gamma_3$	Γ_3 (expt)		Γ_3^0 (MeV)	Γ_1 (expt)		Γ_1^0 (MeV)
				(MeV)	(MeV)		$\Delta\Gamma_1/\Gamma_1$	(MeV)	
Er^{164}	10°	0.28	0.55	2.8	1.85	0.22	5.2	4.2	
Ho^{165a}	19°	0.28	0.55	2.8	1.85	0.22	5.2	4.2	
Ta^{181b}	15°	0.23	0.50	4.5	3.00	0.30	9.5	7.3	

^a See Ref. 6.

^b E. G. Fuller and B. Hayward, Phys. Rev. Letters 1, 1507 (1958).

In elastic scattering the broadenings due to β vibrations are $\Delta\Gamma_1 = 28\%$, $\Delta\Gamma_3 = 20\%$, and to β and γ vibrations combined $\Delta\Gamma_1' = 36\%$, $\Delta\Gamma_3' = 30\%$. These results corroborate with the remark made before: while Er^{164} , because of its strong intrinsic deformation, gives large broadenings in the lower line, the γ -unstable nucleus Os^{188} leads to large broadenings in the higher energy resonance. These relative effects of β and γ vibrations on the two resonances are again observed in the magnitudes of the probabilities of transitions to β and γ levels.

In conclusion, the contribution from shape oscillations seems to be large enough to give an appreciable broaden-

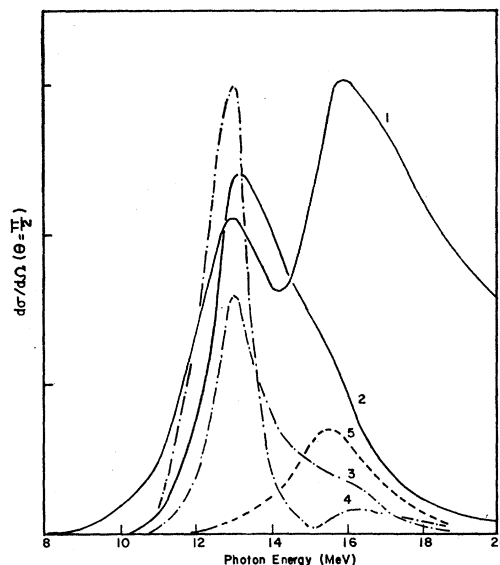


FIG. 13. Relative magnitudes of the probabilities of transition to different states of Os^{188} at 90° . Curves 1 and 2 correspond to the two lowest states of the ground-state band; curves 3 and 4 to the two lowest states of β rotational band; and curve 5 to the lowest γ vibrational level; the last three curves being normalized by a factor of 10.

ing to the original resonance width, which is due to the damping of the dipole motion. Thus the experimental values of the resonance widths, which measure both of these effects, cannot be applied without corrections to the zeroth-order terms in β and γ of such quantities as $A(\beta, \gamma)$. It is easy to estimate for these terms the widths corresponding to the nuclear static shape from the known values of the width broadenings. A few examples are shown in Table III.

In Table III, we are rather conservative in making the estimates of the relative width broadening, $\Delta\Gamma/\Gamma$, by using the experimental value of the width instead of its value corresponding to the static shape of the nucleus which, in general, is smaller. Moreover, for a smaller experimental width, the ratio $\Delta\Gamma/\Gamma$ will increase further, which, in effect, is the case of erbium for example: in Ref. 4, the authors use $\Gamma_3 = 2$ MeV and $\Gamma_1 = 4$ MeV to fit the experimental data. In numerical calculations, the zeroth-order size and width of the resonances depend on the data we use. Relative magnitudes and width broadenings should, however, remain unchanged for a given nucleus. In particular, we expect that the width broadening rather than the width itself varies systematically with nuclear deformation.

ACKNOWLEDGMENT

We would like to acknowledge several interesting and fruitful discussions with Dr. Peter Axel.